Note di Matematica ISSN 1123-2536, e-ISSN 1590-0932
Note Mat. **37** (2017) suppl. 1, 1–17. doi:10.1285/i15900932v37suppl1p1

Rao-Geodesic distance on the generalized gamma manifold: Study of three sub-manifolds and application in the Texture Retrieval domain

Zakariae Abbad
LIM Laboratory, USMBA University
Faculty of sciences Dhar El-Mehraz BP 1796 Atlas 30000, Fez Morocco
zakariaeabbad@gmail.com

Ahmed Drissi El Maliani
LIM Laboratory, USMBA University
Faculty of sciences Dhar El-Mehraz BP 1796 Atlas 30000, Fez Morocco
maliani.ahmed@gmail.com

Said Ouatik Alaoui
LIM Laboratory, USMBA University
Faculty of sciences Dhar El-Mehraz BP 1796 Atlas 30000, Fez Morocco
s_ouatik@yahoo.com

Mohammed El Hassouni
LRIT URAC 29, Faculty of Sciences, Mohammed V University in Rabat, Morocco
mohamed.elhassouni@gmail.com

Received: 28-07-2016; accepted: 04-11-2016.

Abstract. Texture retrieval is a very challenging issue that combines two major tasks, feature extraction (FE) and similarity measurement (SM). The FE step consists of computing some texture characteristics that, even small in size, describe perfectly the texture content by using stochastic models like Gaussian or non-Gaussian (Gamma, Weibull,...) distributions. The estimated parameters will form the vector of characteristics of the texture. Secondly, the SM step consists of deriving a distance on the chosen model manifold, in order to find the closest textures of a query using their characteristic vectors. In this context, the commonly used similarity measure is the Kullback-leibler divergence (KLD). Nevertheless, KLD is not a distance since it does not satisfy symmetry and triangular inequality properties. In this paper we propose Geodesic distance (GD) as a similarity measure on the Generalized Gamma (GG) manifold, in order to illustrate the importance of geometric reasoning in the image retrieval field. The principle idea is the use of the distances between the probability distributions in precise manner through the GD, as an application in the SM between the texture images which are represented by the parameters of the probability distributions. And that can be a good illustration of the value of the Riemannian geometry through statistical manifold in an applied field such as the texture retrieval. Generalized Gamma is a three parameters distribution that covers Gamma, Weibull and Exponential models as special cases, which allowed the modeling of a wide range of texture families. We take advantage of this property in order to make a prior study of the GD for the Gamma, Weibull and Exponential sub-manifolds due to the cumbersomeness of deriving GD for the generalized gamma directly. Experiments are carried out considering texture retrieval in the domains of dual tree complex wavelet transform and steerable pyramid transform, using the Vistex texture database. Results show that GD achieves performances that are close or higher to KLD for the three sub-manifolds, which is of a great interest since GD is a Riemannian metric contrary to KLD.

Keywords: Information geometry, Geodesic distance, Statistical manifold, KLD, CBIR, wavelet transformation

MSC 2010 classification: primary 68Q87, secondary 68U10

Introduction

The research of visually similar content is a central theme in the field of image retrieval. In the past, numerous methods have been proposed to identify similar visual content of the color point of view, texture and shape. The measured characteristics (based on the statistical models, for example see the work of Do and Vetterli[18] and the work of Allili [2]) of an image are grouped into a vector. The similarity between two images can then be measured with a metric defined on the vector space thus defined. The images are considered similar if the distance between them is small. For this, the complexity of calculating the distance must be reasonable since the research task is performed in real time.

In the literature there is several metrics (distance or divergence) between probability distributions that has been defined, such as the Minkowski distance and the Kullback-Leibler Divergence (KLD). In this paper we use the Rao-Geodesic Distance, which is a natural distance measure on statistical manifolds. Knowing that, distances between probability distributions play a critical role in problems of statistical inference and in practical applications to study the relations between a given set of data. A statistical model is defined by a family of probability distributions, usually qualified by a set of continuous parameters known as parameters. These parameters have geometrical properties that are produced by the local information contents and compotitions of the distributions. Starting from Fisher's main work [8] in 1925, the study of these geometrical properties has become widespread in the statistical literature. In 1945, Rao [20] introduced a Riemannian metric as the Fisher information matrix over the parameter space of a parametric family of probability distributions and suggested the geodesic distance caused by the metric as a measure of dissimilarity/similarity between two probability distributions. In the Riemannian geometry the homologue of straight lines are the geodesics, which are the most direct path and shortest distance between two points on the statistical manifold, that they represent two probability distributions. (For an introduction to differential geometry and Riemannian geometry the reader may refer to [23] and [15]).

The Riemannian manifold and the geodesic distance concepts were used in many application fields of computer sciences such as: computer vision and im-

age processing, such as the Fisher-Rao Riemannian metric for Shape Analysis [1], where they use the Fisher geodesics to compute the distance between 2D corpus callosum shapes. Riemannian Priors on the Univariate Normal Model for the image classification [21], where they applyed the new prior distributions on the univariate normal model based on the Riemannian geometry of the univariate normal model the classification. These concepts were also used for color texture classification as in [6]. Our aim is to calculate the Rao geodesic distance of the Generalized Gamma (GG) manifold, motivated by the generecity and the flexibility of the GG distribution. This latter encompasses a variety of well known statistical models, and contains an additional shape parameters, which helps to enhance retrieval and/or classification processes. However, resolving the GG geodesic equations seems a cumbersome task. For this, as a first step of the derivation of Rao geodesic distance in the case of generalized gamma manifold, in this work, we present a case study on three sub-manifolds of the GG manifold, namely the Weibull sub-manifold, the Gamma sub-manifold and the Exponential sub-manifold. The sub-manifolds are deduced by fixing parameters of the GG distributions, which is a common method of deriving GD for statistical manifolds (see [10], and [19]). The study is carried out in the image retrieval domain (and exactly in the similarity measurement step) as an application of the Riemannian manifold and the geodesic distance concepts. The results obtained by the geodesic distance as similarity measurement are compared with the Kullback-Leibler divergence, which is popular distance in the image retrieval domain, but it is not symmetric and does not satisfy the triangle inequality.

The outline of this paper is as follows. In the next section, we set up the first step in image retrieval system which is the Feature Extraction step (FE), where we deal with our images in the wavelet domain, then in the section 2 we present the GG sub-manifolds. In section 3, Rao-Geodesic distance is provided for the three sub-manifolds. In Section 4, experimental results are conducted on the VisTex texture database in order to evaluate the GD performance. Section 5 concludes with some discussions.

1 The wavelet domain

A wavelet is a small wave (or wave) with limited time, which has the ability to describe the time-frequency plane, with atoms of different time brackets. It is an appropriate tool for the analysis of non-stationary or transient phenomena, so the wavelet domain is suitable for representing our images, of course there is another signal analysis domains that can represents the images such as the Fourrier transform, but the scope of this article does not allow us to quote the advantages of the wavelet transform domain compared to the fourrier transform

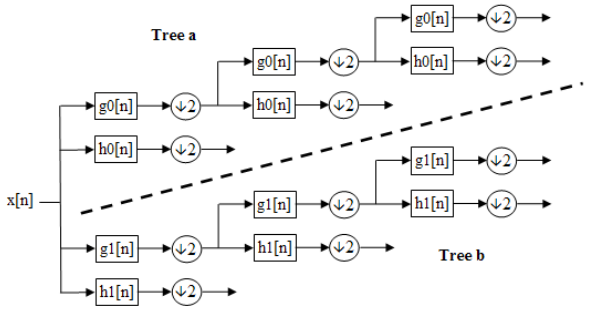

Figure 1. Diagram of a wavelet transform DTCWT.

domain. Among a variety of wavelet transforms in the litterature, in this article we will focus just on the Dual-tree complex wavelet transform (DTCWT), and the Steerable Pyramides (SP).

1.1 The Dual-tree complex wavelet transform (DTCWT)

Complex wavelet transform (CWT) is an expansion of the discrete wavelet transform (DWT) [13]. It provides multi-resolution and accurate representation of the image. The Complex Wavelet Transform Dual Tree (DTCWT) provides the transform of a signal by employing two DWT decompositions (tree a and the tree b, see the Figure 1). It is possible for the DTCWT to produce on the first tree real coefficients and in the other tree imaginary coefficients.

The DTCWT was developed to integrate the adequat properties of the Fourier transform in the wavelet transform, and it was used in the image processing domain such as in [25] and [14]. As the name implies, two trees bank of parallel filters, wavelet, are used, one to generate the real part of complex wavelet coefficients: real tree and the other for generating the imaginary part of the coefficients complex wavelet: imaginary tree.

1.2 The Steerable pyramides (SP)

The steerable pyramid algorithm is an invertible multi-scale image transform [7], it breaks down an image into oriented and band-pass filtered the components at different scales. It has useful shiftability properties in both rendering and rotation [4]. As Mallat inroduces his algorithm of the discrete wavelet transform (DWT) [13], the SP transform decomposes an image into a set of scaled component images from which the original can be rebuilt. The SP sub-samples the image at each step of iteration, generating gradually half-sized images. Con-

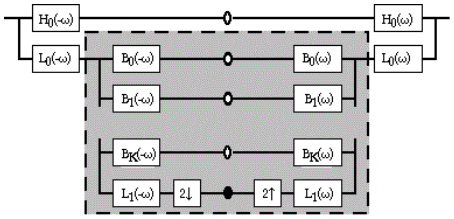

Figure 2. Block diagram of pyramid decomposition.

trary to the DWT, the SP avoids aliasing when sub-sampling [7]. Also unlike the DWT, it is shift and invariant, owing to the absence of aliasing in the down-sampling process. One must choose the order of the derivative upon which the steerable pyramid transform is based. The number, k, of orientation bands at each scale is one more than the order of the derivative. The transform is over-complete by the factor 4k/3.

The block diagram in figure 2 shows that the image is divided into low and highpass subbands, using filters L0 and H0. The lowpass subband is then separated into a series of oriented bandpass subbands and a lowpass subband. This lowpass subband is sub-sampled by a factor of 2 in the X and Y directions. The recursive construction of a pyramid is obtained by inserting a copy of the shaded portion of the diagram at the location of the solid circle.

2 The sub-cases of the Generalized Gamma manifold

Based on the previous chapter, we focus on the characterization of textures in the wavelet domain by probabilistic stochastic models, specifically by using the Generalized Gamma distribution. In reality, we are trying to modeling the histograms of the coefficients derived from the DTCWT or the SP (see the Figure 3) by the GG probability density function (pdf).

The Generalized Gamma distribution (GG) has been studied and applied in different fields, such as speech spectra [22] and stock return modeling [11], it was first introduced by Stacy [24] and then applied in the texture retrieval by Choy [5]. The probability density function of the GG considered is given by:

$$f(x;\theta) = \frac{\beta x^{\beta\lambda-1}}{\alpha^{\beta\lambda}\gamma(\lambda)} e^{-(\frac{x}{\alpha})^{\beta}} \tag{1}$$

$\theta = (\alpha, \beta, \lambda)$ denotes the parameter set, $\alpha > 0$; $\beta > 0$ and $\lambda > 0$ are the scale, shape and index shape parameters respectively; $\gamma(.)$ is the standard Gamma

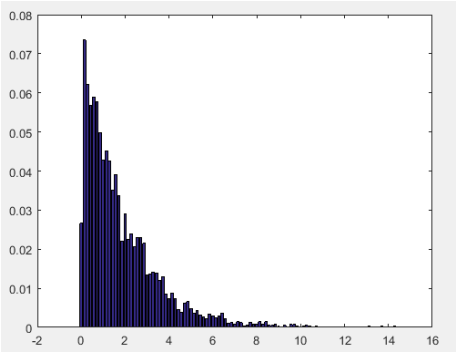

Figure 3. Wavelet subband coefficient histogram.

function defined by: $\gamma(z) = \int_0^{+\infty} e^{(-t)} t^{(z-1)} dt$, $z > 0$. Note that (1) is reduced to the Gamma function when $\beta = 1$, when $\alpha = 1$ we are in the case of the Weibull distribution and when $\alpha = \beta = 1$, we have the exponential distribution. And this is a proof that the GG model covers a wide variety of frequently used distribution such as: the gamma, the weibull and the exponential distributions, that compose our sub-cases study.

2.1 The Gamma distribution

The probability density function using the scale-shape parametrization is:

$$f(x; \alpha, \beta) = \frac{x^{\beta-1}}{\alpha^{\beta}\gamma(\beta)} e^{-(\frac{x}{\alpha})} \tag{2}$$

where $\gamma(.)$ is the standard Gamma function. The Gamma parameters (α and β) can be estimated by the maximum likelihood estimation (MLE), by solving this equation:

$$\hat{\theta} = \arg\max_{\theta} \log \prod_{i=1}^{n} f(x_i; \alpha, \beta) \tag{3}$$

and sloving the equation (3) leads us to the following system of equations:

$$\hat{\alpha} = \frac{1}{n\hat{\beta}} \sum_{i=1}^{n} x_i \quad , \quad \log(\hat{\beta}) - \frac{\gamma\prime(\hat{\beta})}{\gamma(\hat{\beta})} = \log(\frac{1}{n}\sum_{i=1}^{n} x_i) - \frac{1}{n}\sum_{i=1}^{n} log(x_i) \tag{4}$$

2.2 The Weibull distribution

The probability density function using the scale-shape parametrization is:

$$f(x;\alpha,\lambda) = \frac{\beta}{\alpha}(\frac{x}{\alpha})^{k-1}e^{-(\frac{x}{\alpha})^{\beta}} \tag{5}$$

where $\gamma(.)$ is the standard Gamma function. To estimate the parameters of the Weibull distribution (α and λ), the MLE give us the following system of equations to solve:

$$\hat{\lambda}^k = \frac{1}{n}\sum_{i=1}^{n} {x_i}^k \quad , \quad \hat{k}^{-1} = \frac{\sum_{i=1}^{n} {x_i}^k \ln(x_i)}{\sum_{i=1}^{n} {x_i}^k} - \frac{1}{n}\sum_{i=1}^{n}\ln(x_i) \tag{6}$$

2.3 The Exponential distribution

The probability density function using the one parametrization is:

$$f(x;\lambda) = \lambda e^{-\lambda x} \tag{7}$$

here $\lambda > 0$ is the parameter of the distribution, often called the rate parameter. The maximum likelihood estimate for the rate parameter is:

$$\hat{\lambda} = \frac{1}{\frac{1}{n}\sum_{i=1}^{n} x_i} \tag{8}$$

3 The Geodesic Distance on statistical manifolds

Statistical manifolds are representations of smooth families of probability density functions that allow differential geometry to be applied to problems in stochastic processes and information theory. We model a family of probability distribution functions given by a set of parameters. In other words, we consider each distribution as a point on a Riemannian manifold.

If we want to see the FE step from a mathematical point of view, we can say that the images in the database are considered as elements of the manifold and each image is considered as point on the statistical manifold (as the Figure 4 shows). In our case, we are modeling our images by the set of parameters that had been estimated in the Feature Extraction step (FE), in order to measure the distance between our images, represented by their set of parameters, in the Similarity Measurement step (SM), (for more details about the image retrieval systems see the Experimental Results section)

Rao [20] proposed a method (Rao-Geodesic distance) for measuring distances between distributions of a parametric family, all of whose members satisfy certain regularity conditions(see [3]). The measure is based on a metric of

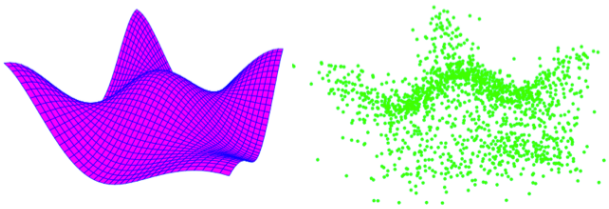

Figure 4. Statistical manifold.

a Riemannian geometry, the metric being in terms of the elements of the information matrix for the family [3]. In information geometry [23], it is well known that a parametric model $\{p_\theta; \theta \in \Theta\}$, where $\Theta \subset R^r$, can be equipped with a Riemannian geometry, determined by Fishers information matrix:

$$g_{ij}(\theta) = E\left\{\frac{\partial \ln p(X|\theta)}{\partial \theta_i}\frac{\partial \ln p(X|\theta)}{\partial \theta_j} \mid \theta\right\} \tag{9}$$

with (i, j = 1, 2, ..., r), which we calculated in the case of the GG by the following matrix:

$$I(\alpha,\beta,\lambda) = \begin{pmatrix} \frac{\lambda\beta^2}{\alpha^2} & \frac{-1}{\alpha}(\lambda\psi(\lambda)+1) & \frac{\beta}{\alpha} \\ \frac{-1}{\alpha}(\lambda\psi(\lambda)+1) & \frac{1}{\beta^2}[1+\lambda\psi(1,\lambda)+\lambda\psi(\lambda)^2+2\psi(\lambda)] & \frac{-\psi(\lambda)}{\beta} \\ \frac{\beta}{\alpha} & \frac{-\psi(\lambda)}{\beta} & \psi(1,\lambda) \end{pmatrix}$$

where $\psi(.)$ is the digamma function defined by: $\psi(z) = \frac{\gamma\prime(z)}{\gamma(z)}$, and the $\psi(m,z)$ is the polygamma function defined by: $\psi(m,z) = \frac{d^{(m)}}{dz^m}\psi(z)$.

Indeed, assuming that $g_{ij}(\theta)$ is strictly positive definite, for each $\theta \in \Theta$, a Riemannian metric on Θ is defined by:

$$ds^2(\theta) = \sum_{i,j=1}^{r} g_{ij}(\theta)d\theta^i d\theta^j \tag{10}$$

Once the Riemannian metric Equation (10) is introduced, given two probability measures P_{θ_1} and P_{θ_2} which belong to the statistical model, the Rao distance between P_{θ_1} and P_{θ_2} is defined as the Riemannian distance between $\delta(\theta_1,\theta_2) \in \Theta$, by the following formula:

$$\delta(\theta_1,\theta_2) = \mid \int_{t_1}^{t_2} [\sum_{i,j=1}^{r} g_{ij}(\theta)\frac{d\theta^i}{dt}\frac{d\theta^j}{dt}]^{\frac{1}{2}}dt \mid \tag{11}$$

In particular, among the curves between θ_1 and θ_1, which interest us is the one that represents the minimum distance between these two points. We call it the Geodesic, and it is given as a solution to differential equations, called the Euler-Lagrange equations (or the geodesic equations) :

$$\ddot{\theta^k}(t) + \sum_{i,j} \Gamma^k_{ij}[\theta(t)]\dot{\theta^i}(t)\dot{\theta^j}(t) = 0 \tag{12}$$

where the $\Gamma^k_{\mu\upsilon}$ is the Christoffel symbols of the second kind, that is defined by:

$$\Gamma^k_{\mu\upsilon} = \frac{1}{2}\sum_{\rho} g^{k\rho}\left(\frac{\partial g_{\upsilon\rho}}{\partial\theta^\mu} + \frac{\partial g_{\mu\rho}}{\partial\theta^\upsilon} - \frac{\partial g_{\mu\upsilon}}{\partial\theta^\rho}\right) \tag{13}$$

and $g^{\mu\upsilon}$ denotes the components of the inverse metric. The geodesic equations are defined in the case of the GG as follows:

$$\begin{cases} \ddot{\alpha} + \Gamma^\alpha_{\alpha\alpha}\dot{\alpha}^2 + 2\Gamma^\alpha_{\alpha\beta}\dot{\alpha}\dot{\beta} + 2\Gamma^\alpha_{\alpha\lambda}\dot{\alpha}\dot{\lambda} + 2\Gamma^\alpha_{\beta\lambda}\dot{\beta}\dot{\lambda} &= 0 \\ \ddot{\beta} + \Gamma^\beta_{\alpha\alpha}\dot{\alpha}^2 + \Gamma^\beta_{\beta\beta}\dot{\beta}^2 + \Gamma^\beta_{\lambda\lambda}\dot{\lambda}^2 + 2\Gamma^\beta_{\alpha\lambda}\dot{\alpha}\dot{\lambda} + 2\Gamma^\beta_{\beta\lambda}\dot{\beta}\dot{\lambda} &= 0 \\ \ddot{\lambda} + \Gamma^\lambda_{\alpha\alpha}\dot{\alpha}^2 + \Gamma^\lambda_{\beta\beta}\dot{\beta}^2 + \Gamma^\lambda_{\lambda\lambda}\dot{\lambda}^2 + 2\Gamma^\lambda_{\alpha\beta}\dot{\alpha}\dot{\beta} &= 0 \end{cases}$$

As already stated, before solving equations for the general GG case, in this paper, we provide a case-study by fixing different GG parameters. This lead us to a sub-manifold GD study.

3.1 The Geodesic distance on Gamma sub-manifold

The Rao-Geodesic distance has been computed for several statistical models, see Atkinson and Mitchell [3], Mitchell and Krzanowski [9]among others. There are some statistical models, such as Generalized Gaussian, for which a closed form of the Rao distance is not available, in which cases a numerical approach may be appropriate. Nevertheless, for distributions that lie infinitesimally close on the probabilistic manifold, it can be proved that the KLD equals half of the squared GD between the distributions. It follows that locally [12]:

$$GD(f_{\theta_1}, f_{\theta_2}) \approx \sqrt{2SKLD(f_{\theta_1}, f_{\theta_2})} \tag{14}$$

with:
$SKLD(f_{\theta_1}, f_{\theta_2}) = KLD(f_{\theta_1}, f_{\theta_2}) + KLD(f_{\theta_2}, f_{\theta_1})$ and

$$KLD(f(x;\alpha_1,\beta_1), f(x;\alpha_2,\beta_2), f_{\theta_2}) = (\alpha_1-\alpha_2)\psi(\alpha_1) - \log\gamma(\alpha_1) + \log\gamma(\alpha_2) + \alpha_2(\log\beta_2 - \log\beta_1) + \alpha_1\frac{\beta_1-\beta_2}{\beta_2} \quad (15)$$

where $\psi(\alpha)$ is the digamma function.

3.2 The Geodesic distance on Weibull sub-manifold

For the case of the Weibull distribution a closed form of the Rao distance is available, and it is defined as it follows [17]:

$$GD(f_{\theta_1}, f_{\theta_2}) = \frac{\pi}{\sqrt{6}}\log\frac{1+K}{1-K} \quad (16)$$

where: $K = \left(\frac{[\log(\frac{\beta_2}{\beta_1}) - a\frac{(\lambda_2-\lambda_1)}{\lambda_2\lambda_1}]^2 + b^2\frac{(\lambda_2-\lambda_1)^2}{\lambda_2^2\lambda_1^2}}{[\log(\frac{\beta_2}{\beta_1}) - a\frac{(\lambda_2-\lambda_1)}{\lambda_2\lambda_1}]^2 + b^2\frac{(\lambda_2+\lambda_1)^2}{\lambda_2^2\lambda_1^2}}\right)^{\frac{1}{2}}$ and $a = 1-\gamma, b = \frac{\pi}{\sqrt{6}}$ (γ is the Euler constant).

3.3 The Geodesic distance on Exponential sub-manifold

According to the Atkinson and al. paper [3], the closed form of the Rao distance on the Exponential manifold isdefined by:

$$GD(f_{\theta_1}, f_{\theta_2}) = \mid \log\left(\frac{\lambda_1}{\lambda_2}\right) \mid \quad (17)$$

4 Experimental Results

The Content-Based Image Retrieval (CBIR) is a technique to search for images based on their visual characteristics. Images are conventionally described by descriptors such as texture, color or shape.

The general principle of content-based image retrieval has two stages (Figure 5). During a first phase, which is the Feature Extraction (FE) (offline mode), the signatures of the images is calculated and stored in a database. In the second phase, which is the Similarity Measurement (SM), the research is conducted online. The user submits an image as a query. The system calculates the signature according to the same manner as during the first phase of indexing. Thus, this

signature is compared to all previously stored signatures to bring back the most similar image to the query.

In this section, experiment is conducted to test the effectivenesse of the geodesic distance as a similarity measure for CBIR. We used database Vistex [16] which is a collection of texture images. The purpose of Vistex is to provide texture images which are representative of actual conditions, and contains 40 color classes textures, and in each class has 16 different images.(See the Figure 6)

First, we take each texture image in the database and we turn it to the gray-level(because we need only the texture descriptor).Then each image is decomposed via the Dual Tree Complex Wavelet Transform (DTCWT). After that, each sub-band is represented via the parameters of the generalized gamma model. The parameters of each sub-band of the image are then concatenated to represente the image.

Table 1 shows the average of the retrieval for the three sub-manifolds com-

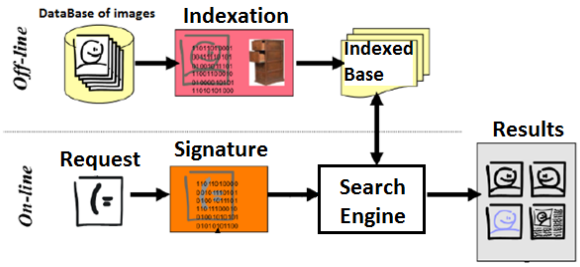

Figure 5. Architecture of the CBIR system.

Figure 6. 40 texture classes from the Vistex database.

	Level 1 (DTCWT)	Level 2 (DTCWT)	Level 3 (DTCWT)
Gamma + GD	71.3281	78.2910	80.9375
Gamma + KLD	72.0801	78.6816	80.7813
Weibull +GD	72.4414	78.9648	81.6406
Weibull +KLD	72.7832	78.6328	80.8691
Exponential + GD	58.9648	68.8574	74.1504
Exponential + KLD	61.2305	71.2891	76.4063

Table 1. The retrieval rate of the three sub-manifolds modeling the DTCWT coefficients combined with the Geodesic Distance(GD) or the KLD

	Level 1(SP)	Level 2(SP)
Gamma + GD	64.2773	74.5801
Gamma + KLD	64.0234	74.5996
Weibull +GD	65.3125	75.6055
Weibull +KLD	64.3750	74.8926
Exponential + GD	54.1699	65.5371
Exponential + KLD	55.5273	67.3438

Table 2. The retrieval rate of the three sub-manifolds modeling the SP coefficients combined with the Geodesic Distance(GD) or the KLD

bined with the Geodesic Distance(GD) and the KLD. We observe that the (Gamma + GD) achieves higher retrieval rate in the level 3 of decomposition(80.9375). The (Weibull + GD)has shown also higher retrieval rate from the second level of decomposition (78.9648 and 81.6406). Regarding, the (Exponential + GD), we notice a lower retrieval rate compared to the (Gamma + GD) and the (Weibull + GD), and this is explained by, that the Exponential distribution has single parameter (more we have the parameters, better we can modelize shapes).

In the second experiment, instead of decomposing the bands of each image via the DTCWT, we will use the Steerable Pyramids (SP) decomposition following the same way of the first experiment.

The table 2 shows the average of the retrieval for the three sub-manifolds combined with the Geodesic Distance(GD) and the KLD. We observe that for the (Gamma + GD) achieves retrieval rate in the level 2 (74.5801) of decompositon which is close to the retrieval rate of the (Gamma + KLD). The (Weibull + GD)has shown higher retrieval rate compared to the (Weibull + KLD). As it is the case for the Exponential distribution (GD or KLD) in the Table 1, we notice a lower retrieval rate compared to the Gamma and the Weibull.

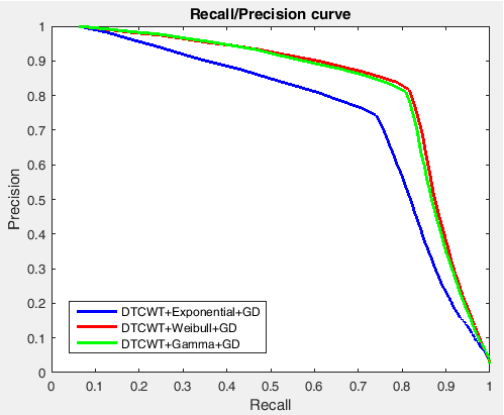

Figure 7. Recall/Precision curves obtained using a GG sub-manifold and the geodesic distance considering DTCWT transforms.

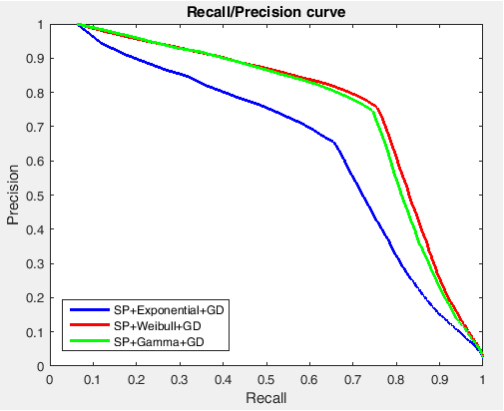

Figure 8. Recall/Precision curves obtained using a GG sub-manifold and the geodesic distance considering SP transforms.

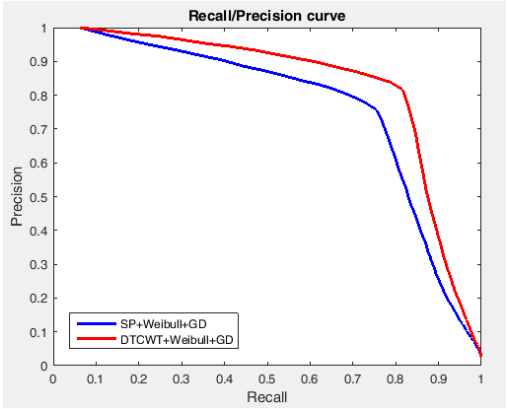

Figure 9. Recall/Precision curves obtained using a GG sub-manifold (Weibull) and the geodesic distance considering SP and DTCWT transforms.

Furthermore, Figure 7 shows the recall/precision curves for the sub-cases of the Generalized Gamma distribution combined with the DTCWT decomposition (Level 3). We note that the "DTCWT+Weibull+GD"has the highest performance among the other methods, which is already proved by the experiment results int the table 1.

The same remark is for Figure 8, that shows the recall/precision curves for the sub-cases of the Generalized Gamma distribution combined with the SP decomposition (Level 2). The "SP+Weibull+GD"has the highest performance among the other methods, which is already proved by the experiment results int the table 2.

In the Figure 9, we take the most powerful method in the Figure 7 which is the "DTCWT+Weibull+GD" and the most performante method in the Figure 8 which is the "SP+Weibull+GD" to see the method that has the highest performance among the methods existing in the two figures (7 and 8). We notice that the "DTCWT+Weibull+GD" achieves high performance, which shows that the DTCWT is more suitable to represent the spectral content of textures.

5 Conclusion

In this paper, we have studied the use of the Rao-Geodesic distance as a similarity measurement on the GG manifold. For this a parameter fixing technique helps to conduct a case study on three sub-manifolds of the GG manifold.

The experimental results show that GD achieves performances that are close or higher to the common Kullback-Leibler Divergence. However, as it is known, the advantage of GD is that it fulfills the distance properties contrary to KLD (symmetry and triangular innequality properties). Our future work, will be devoted to the derivation of the Rao geodesic distance of the GG manifold in the general case.

Acknowledgements. We acknowledge helpful conversations and guidance of Mohamed Tahar Kadaoui Abbassi, who is a Professor within the mathematical departement of the Faculty of sciences Dhar El Mahraz in fez.

References

[1] P. Adrian and A. Rangarajan, *Shape Analysis Using the Fisher-Rao Riemannian Metric: Unifying Shape Representation and Deformation*. Indian Journal of Statistics, (2006).

[2] M. S. Allili, *Wavelet Modeling Using Finite Mixtures of Generalized Gaussian Distributions: Application to Texture Discrimination and Retrieval*. IEEE TRANSACTIONS ON IMAGE PROCESSING, (2012).

[3] C. Atkinson and A. F.S.Mitchell, *The Mahalanobis distance and elliptic distributions*. Biometrika, (1985).

[4] R. Bamberger and M. Smith, *A Filter Bank for the Directional Decomposition of Images: Theory and Design*. IEEE TRANSACTIONS SP-40, (1992).

[5] S. K. Choy AND C. S. Tong. *Statistical Wavelet Subband Characterization Based on Generalized Gamma Density and Its Application in Texture Retrieval*. IEEE Signal Process, (2009).

[6] A. D. ElMaliani, M. ElHassouni, Y. Berthoumieu, and D. Aboutajdine, *Color Texture Classification Using Rao Distance Between Multivariate Copula Based Models*. Computer Analysis of Images and Patterns, (2011).

[7] E.P.Simoncelli and W.T.Freeman, *The Steerable Pyramid: A Flexible Architecture for Multi-scale Derivative Computation*. Proc. ICIP-95, (1995).

[8] R. A. Fisher, *Theory of statistical estimation*. Proceedings of the Cambridge Philosophical Society, (1925).

[9] A. F.S.Mitchell and W. Krzanowski, *Rao's Distance Measure*. The Indian Journal of Statistics, (2002).

[10] V. Geert and P. Scheunders, *The Geometry of Multivariate Generalized Gaussian Models Part I: Metric and Geodesic Equations*. IEEE TRANSACTIONS ON IMAGE PROCESSING, (2009).

[11] O. Gomes AND C. Combes AND A. Dussauchoy *Four-Parameter Generalized Gamma Distribution Used for Stock Return Modeling*. IMACS Multiconference on Computational Engineering in Systems Applications, (2006).

[12] S. Kullback, *Information Theory and Statistics*. Dover Publications, 1968.

[13] S. Mallat, *A Theory for Multiresolution Signal Decomposition: The Wavelet Representation*. IEEE TRANSACTIONS PAMI-11, (1989).

[14] P. Mayuri, T. Shivkumar, Singh, and K.Chaturvedi, *Dual Tree Complex Wavelet Transform (DTCWT) based Adaptive Interpolation Technique for Enhancement of Image Resolution*. International Journal of Computer Applications, (2013).

[15] K. Michael and W. John, *Differential Geometry and Statistics*. Springer Science+Business Media, B.V, 1993.

[16] MIT, *Vision texture*, jun 2009. (`http://vismod.media.mit.edu/vismod/imagery/VisionTexture/`).

[17] J. M.Oller, *Information Metric for Extreme Value and Logistic Probability Distributions*. The Indian Journal of Statistics, (1987).

[18] M. N.Do and M. Vetterli, *Wavelet-Based Texture Retrieval Using Generalized Gaus- sian Density and KullbackLeibler Distance*. IEEE TRANSACTIONS ON IMAGE PROCESSING, (2002).

[19] H. Rami, L. Belmerhnia, A. D. El Maliani, and M. El Hassouni, *Texture retrieval using mixtures of generalized Gaussian distribution and Cauchy-Schwarz divergence in wavelet domain*. Elsevier Science: Image Communication, Volume 42 Issue C, (2016).

[20] C.R. Rao. *Information and the accuracy attainable in the estimation of statistical parameters*. Calcutta Math, (1945).

[21] S. Salem, L. Bombrun, and Y. Berthoumieu, *New Riemannian Priors on the Univariate Normal Model*. The Entropy Journal, (2014).

[22] J. W. Shin AND J. H. Chang AND N. S. Kim *Statistical Modeling of Speech Signals Based on Generalized Gamma Distribution.* IEEE Signal Process, (2005).

[23] A. Shun-chi, *Mehods of Information Geometry.* OXFORD University Press, 1993.

[24] E. W. Stacy. *A Generalization of the Gamma Distribution.* Ann. Math. Statist, (1962).

[25] R. V.Naga, Prudhvi and T.Venkateswarlu, *Denoising of Medical Images Using Dual Tree Complex Wavelet Transform.* 2nd International Conference on Computer, Communication, Control and Information Technology, (2012).